Spin Splitting Induced by Spin-Orbit Interaction in Chiral Nanotubes

L. Chico,[1] M. P. López-Sancho,[2] and M. C. Muñoz[2]

[1]*Departamento de Física Aplicada, Facultad de Ciencias del Medio Ambiente, Universidad de Castilla-La Mancha, 45071 Toledo, Spain*

[2]*Instituto de Ciencia de Materiales de Madrid, Consejo Superior de Investigaciones Científicas, Cantoblanco, 28049 Madrid, Spain*

(Received 14 May 2004; published 18 October 2004)

We show that chiral tubes present spin splitting at the Fermi level in the absence of a magnetic field, whereas achiral tubes preserve spin degeneracy, as evidenced by tight-binding electronic structure calculations with the inclusion of spin-orbit interaction. These remarkably different behaviors of chiral and nonchiral nanotubes have a symmetry origin, which may provide a global explanation to recently reported spin-dependent transport experiments which were in apparent contradiction.

DOI: 10.1103/PhysRevLett.93.176402 PACS numbers: 71.20.Tx, 71.70.Ej, 73.22.–f

Carbon nanotubes (CNTs) constitute a new class of mesoscopic 1D quantum systems [1]. Their unusual electrical properties offer new possibilities for the design and implementation of nanoelectronic devices. Scanned-probe spectroscopy measurements in both single-wall and multiwall nanotubes (NTs) agree overall with the predictions of band structure calculations, which state that NTs can either be metals or semiconductors depending on their diameter and chirality [2]. However, transport experiments in CNTs have posed new open questions that require an explanation going beyond the simplest models [3–8]. For example, single-electron transport experiments [5–8] have evidenced that the role of spin in these quasi-1D systems might be crucial. Thus, CNTs could play an important part in spin-electronic devices, whose operation depends not only on the charge but also on the spin of the conduction electrons. Nonetheless, these transport experiments seem to lead to contradictory results, giving support to the existence of different spin ground states in CNTs. By analyzing the spin directions of successive electrons entering a bundle of NTs at low magnetic fields, the expected spin alternation was found [5]. Such behavior was also found in carbon nanotube quantum dots [6] and could be explained by a simple shell-filling model. However, measurements performed in isolated NTs showed that consecutive electrons could have the same spin direction, indicating a possible spin polarization of the NT [7]. These authors gave a phenomenological explanation for the parallel spin (PS) sequences, assuming that the capacitance of the NT depends on its many-body quantum state. Another proposed mechanism to interpret this unexpected spin succession was the presence of a nonuniform external potential along the tube axis [9]. Consecutive parallel electrons were also reported in a later work on metallic CNTs [8]. In this case a four-electron periodicity for electron addition was observed compatible with a ground state spin $S = 1$ at most. These results were understood by employing a shell-filling model which incorporates exchange and Coulomb interactions.

The process of electron transport involves the distribution of incoming electron flux among the eigenstates of the system, so the precise knowledge of the energy spectrum of CNTs is essential to understand quantum transport. It is the aim of this Letter to show that chiral CNTs can present spin-split states at the Fermi level in the absence of a magnetic field, as found by electronic structure calculations including spin-orbit interactions. Spin polarization is crucially dependent on the NT symmetry: in chiral NTs spin-orbit (SO) interaction lifts the spin degeneracy, while in achiral NTs, either armchair or zigzag, spin degeneracy remains. The effects of SO coupling have been previously studied in CNTs [10–12]. A continuous $\mathbf{k} \cdot \mathbf{p}$ scheme based on a single p_z orbital at each C atom and neglecting curvature effects predicts that for metallic NTs a small energy gap opens up, but spin splitting is not present around the Fermi energy (E_F) [10]. Band splitting induced by SO coupling has been obtained considering surface curvature effects [11] and in electron spin resonance spectra of achiral NTs derived by low-energy field theory [12,13]. The inclusion of the full NT lattice symmetry, absent in these previous works, turns out to be essential for SO-coupling effects in chiral NTs.

We model the NT by the Slater-Koster [14] empirical tight-binding (ETB) Hamiltonian including sp^3 orbitals, employing the Tománek-Louie parametrization for graphite [15], so the actual discrete nature of the lattice is taken into account. The NT unit cell is generated by rolling up a portion of graphene layer, thus including curvature effects. Although total energy calculations give smaller radii for relaxed NTs, changes in the band structure for the diameters here studied ($d \geq 6$ Å) are negligible [16].

Spin-orbit interaction is caused by the coupling of the spin of a moving electron with an electric field which acts as a magnetic field in the rest frame of the electron. In a crystalline environment the major internal contribution arises from the electron orbital motion in the crystal potential V, and thus its effects are related to the crystal

symmetry. The SO-interaction term in the Hamiltonian is $H_{SO} = \frac{\hbar}{4mc^2}\boldsymbol{\sigma}(\nabla V \times \mathbf{p})$, where $\boldsymbol{\sigma}$ represents the Pauli matrices and $\mathbf{p}$ the electron momentum. The relevant contribution of the crystal potential is close to the atomic cores, so assuming spherical symmetry, $H_{SO} = \lambda \mathbf{L} \cdot \mathbf{S}$, where the SO-coupling constant λ depends on the atomic orbital and $\mathbf{L}$ is the angular momentum of the electron. Within the ETB framework, H_{SO} interaction couples p orbitals on the same atom, and λ can be either greater or smaller than the atomic value [17]. It was assumed long ago [18] that the SO interaction in graphite was reduced with respect to the value for atomic C; thus SO effects have been customarily neglected in graphitelike materials, even though recent measurements are lacking. Low dimensionality, electron-electron interactions, and magnetic fields are shown to induce an enhancement of SO coupling [19]. Therefore, it may turn out that spin-orbit interactions in CNTs could be relevant due to their reduced dimensionality. Furthermore, the SO strength can be controlled by a proper choice of gate potentials [20], as was first proposed for semiconductor heterostructures.

It is our purpose to explore the symmetry dependence of SO interaction in buckytubes, which are known to appear in a variety of geometries and, consequently, they present different symmetries. Calculations have been done with a SO-coupling constant $\lambda = 0.2$ eV for the sake of clarity in the figures; however, its exact value is not known. We have focused on primary metallic nanotubes, i.e., nanotubes which are predicted to be metallic if curvature effects are neglected [21]. To this end, we have calculated the band structure of four different NTs including SO-interaction [22]. The selection regards the diverse types of bands at E_F. Neglecting curvature effects, all primary metallic tubes [23] present a band crossing at the Fermi level. According to it, they can be classified as two types: those that have this crossing at Γ and those that have it at two thirds of the distance from Γ to the zone boundary. We will refer to them as Γ metals and $2/3$ metals, respectively [24]. Armchair (n, n) nanotubes are $2/3$ metals, while zigzag $(n, 0)$ tubes ($n = 3q$, q being an integer) are Γ metals [25]. For symmetry considerations, one can see that the bands of any nanotube are at most fourfold degenerate. Considering spin, the bands crossing at E_F in Γ metals are fourfold degenerate at E_F, whereas the bands that cross at E_F in $2/3$ metals are only doubly degenerate.

First we focus on achiral NTs which possess inversion symmetry: Figure 1 shows the band structures of an armchair (5,5) tube [Figs. 1(a) and 1(b)] and a zigzag (9,0) tube [Figs. 1(c) and 1(d)] calculated around E_F with and without SO interaction. The (5,5) tube is a $2/3$ metal, so its bands around the Fermi level have only spin degeneracy [26]. Figures 1(a) and 1(b) clearly show that this degeneracy is not lifted by SO interaction. However, even though armchair tubes remain metallic after including curvature effects [Fig. 1(a)], the inclusion of SO interaction leads to a small gap opening, barely seen in Fig. 1(b), as predicted by Ando [10].

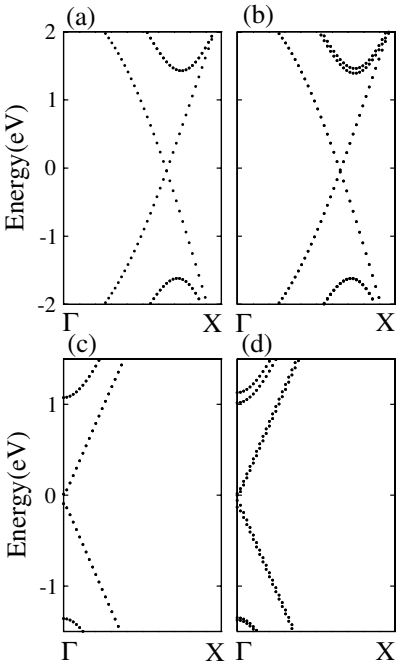

FIG. 1. Band structure calculated around the Fermi level of the achiral tubes: (5,5) armchair tube (a) without and (b) with SO interaction; (9,0) zigzag tube (c) without and (d) with SO interaction.

The zigzag (9,0) tube has been chosen as an example of achiral Γ metal [27]. In Fig. 1(c) we can already see how curvature effects open a small gap in the absence of SO interactions. In Fig. 1(d) it is shown how the inclusion of SO coupling partially removes the degeneracy but, as for the (5,5) tube, the bands around E_F are still twofold degenerate because of spin.

On the other hand, chiral NTs do not have an inversion center and possess spiral symmetry operations. We have chosen the (7,1) and the (9,3) as examples of $2/3$ and Γ metals, respectively [28]. Curvature effects open a small gap at the Fermi energy in both NTs, and slightly shift the Fermi wave vector for the (9,3), which actually has its gap at $\mathbf{k} \neq 0$ value, as can be seen in Fig. 2(c). In contrast to the results shown for armchair and zigzag NTs, SO interaction lifts all degeneracies, even for states which are only doubly degenerate in spin (see Fig. 2). Thus, SO interaction produces an energy splitting between states with different spin orientations in chiral nanotubes. In all tubules the band crossing at E_F is between energy bands of different symmetry, then they respond differently to the SO interaction. This is appreciable in Figs. 1 and 2 since the SO splitting is band dependent.

We have just shown that SO-related effects in NTs have a fundamental symmetry dependence. Even though the SO interaction partially lifts degeneracy in achiral NTs, it

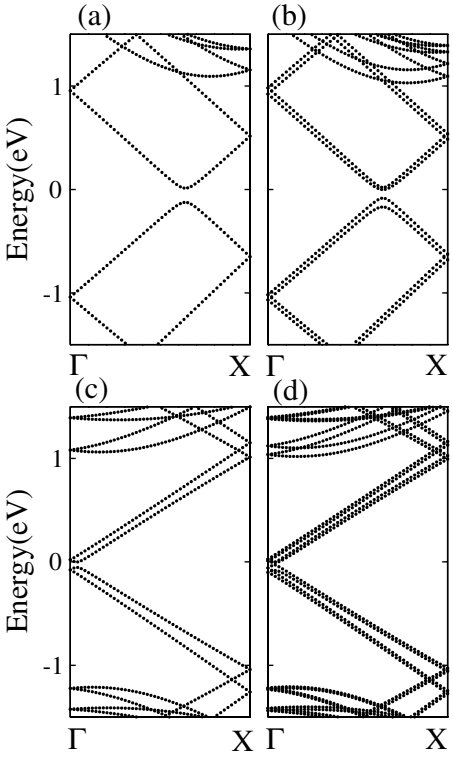

FIG. 2. Same as Fig. 1 for the chiral tubes (7,1) (a),(b) and (9,3) (c),(d).

does not affect the spin degenerate states. This can be understood as follows: Kramers' theorem on time reversal symmetry states that $E_{\mathbf{k},\sigma} = E_{-\mathbf{k},-\sigma}$, where $E_{\mathbf{k},\sigma}$ is the energy of the eigenstate with wave vector $\mathbf{k}$ and spin σ. But if a crystal also has inversion symmetry, that is, $E_{\mathbf{k},\sigma} = E_{-\mathbf{k},\sigma}$, then $E_{\mathbf{k},\sigma} = E_{\mathbf{k},-\sigma}$; i.e., spin degeneracy cannot be removed. But for chiral tubes, because of the lack of inversion symmetry, only the first condition ($E_{\mathbf{k},\uparrow} = E_{-\mathbf{k},\downarrow}$) holds; therefore spin degeneracy is not allowed. This results in an asymmetry in momentum space for the energy branches corresponding to up and down electrons as illustrated in Fig. 3, where the spin-resolved dispersion relation for the (9,3) NT around E_F is represented, showing how electron velocities become dependent on both the spin and the direction of the motion.

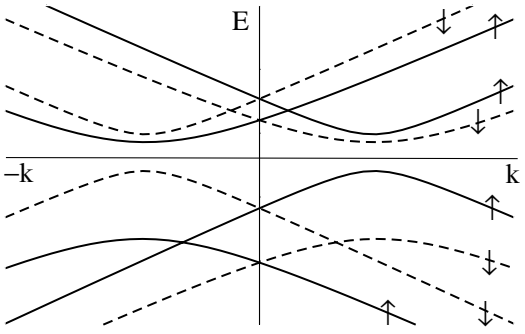

FIG. 3. SO spin-split dispersion relation for the chiral tube (9,3), calculated around the Fermi level in the Γ region of the Brillouin zone (BZ). Arrows indicate the spin polarization of the bands.

In Fig. 4 the spin-resolved density of states (DOS) at $\mathbf{k}_F$ for energies around the Fermi level, with and without SO coupling, are compared for the (5,5) and the (7,1) NTs. In the (5,5) a small gap opens with the SO interaction but no spin splitting is present. Nevertheless, the states are no longer spin eigenstates. The eigenfunctions (not shown here), although with a dominant spin contribution, do not correspond to pure spin states. Thus, as was pointed out by Ando [10], spin scattering is induced even by spin-independent scatterers and impurities can cause spin relaxation. The experimental determination of the SO-induced gap could provide a way to estimate the SO-interaction strength. On the other hand, in the chiral (7,1) NT the SO interaction lifts the degeneracy producing an energy splitting between states with different spin orientation. The bands correspond to spin eigenstates. The motion of electrons with spin up and spin down are completely decoupled. Thus, there is not spin scattering for scatterers having spin-independent potential. In fact, an electron with spin up cannot be scattered into a state with spin down and vice versa. This would explain the

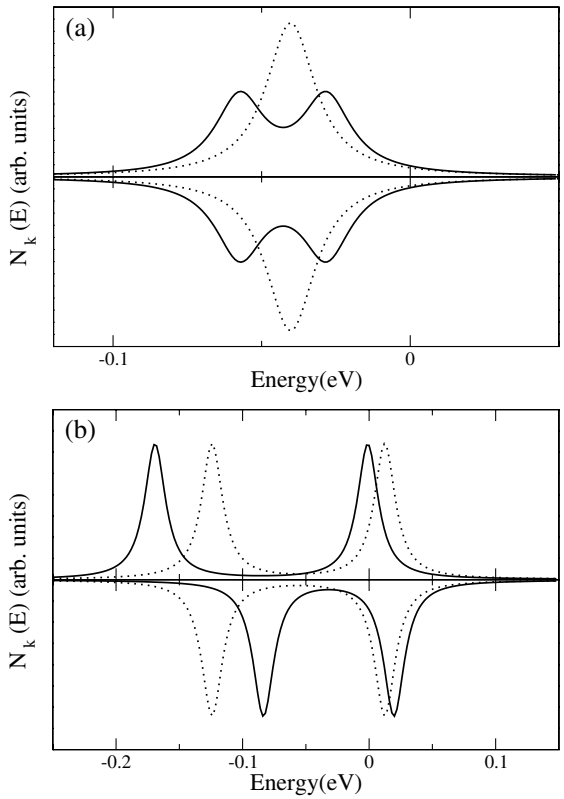

FIG. 4. Spin-resolved DOS at $\mathbf{k}_F$ for (a) the (5,5) nanotube and (b) the (7,1) nanotube, calculated with (solid line) and without (dotted line) SO interaction.

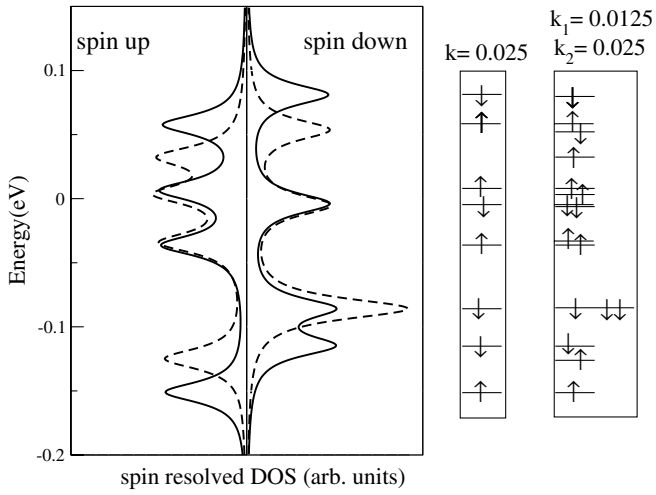

FIG. 5. Spin-resolved DOS for the (9,3) tube at $\mathbf{k} = 0.025$ (solid line) and $\mathbf{k} = 0.0125$ (dashed line) and schematic representation of the sequential ordering of spin-states, considering either one or both $\mathbf{k}$ vectors (see text). Wave vector values are given with respect to the BZ length.

huge (≈ 130 nm) spin-flip scattering length observed for spin-polarized electrons injected into multiwall NT [4].

A finite-length NT has a series of discrete levels arising from the quantized allowed $\mathbf{k}$ values. This, along with the SO-induced spin splitting, can lead to sequences of discrete states with parallel spin. Such effect occurs in chiral NTs at energies around a band gap and whenever there are two bands close in energy with different symmetry, since they respond differently to the SO interaction. To illustrate it, we show in Fig. 5 the sequence of levels corresponding to one particular $\mathbf{k}$ value and that obtained for two values, namely, $\mathbf{k}$ and $\mathbf{k}/2$, which would correspond to the first nonzero quantized $\mathbf{k}$s appearing in a tube of finite length L and $2L$, respectively.

Although we have focused in metallic tubes, SO-induced spin splitting is also present in chiral semiconductor tubes, where SO-related effects are the same. In summary, we have shown that SO interaction removes spin degeneracy in chiral NTs due to the lack of inversion symmetry of the crystal potential, while in achiral NTs spin degeneracy is not lifted. Thus, SO interaction in CNTs presents an intrinsic symmetry dependence. Our results provide a new perspective to the interpretation of spin-polarized transport experiments in CNTs.

This work has been partially supported by the Spanish DGES under Grants No. MAT2002-04095-C02-01, No. MAT2003-04278, and No. MAT2002-04540-C05-03.

[1] R. Saito, G. Dresselhaus, and M. Dresselhaus, *Physical Properties of Carbon Nanotubes* (Imperial College Press, London, 1998).

[2] J. W. G. Wildöer *et al.*, Nature (London) **391**, 59 (1998); T. W. Odom *et al.*, Nature (London) **391**, 62 (1998).

[3] S. Frank *et al.*, Science **280**, 1744 (1998); W. Liang *et al.*, Nature (London) **411**, 665 (2001); J. Kong *et al.*, Phys. Rev. Lett. **87**, 106801 (2001).

[4] K. Tsukagoshi, B. W. Alphenaar, and H. Ago, Nature (London) **401**, 572 (1999).

[5] D. H. Cobden *et al.*, Phys. Rev. Lett. **81**, 681 (1998).

[6] D. H. Cobden and J. Nygård, Phys. Rev. Lett. **89**, 046803 (2002).

[7] S. J. Tans *et al.*, Nature (London) **394**, 761 (1998).

[8] W. Liang, M. Bockrath, and H. Park, Phys. Rev. Lett. **88**, 126801 (2002).

[9] Y. Oreg, K. Byczuk, and B. I. Halperin, Phys. Rev. Lett. **85**, 365 (2000).

[10] T. Ando, J. Phys. Soc. Jpn. **69**, 1757 (2000).

[11] M. V. Entin and L. I. Magarill, Phys. Rev. B **64**, 085330 (2001).

[12] A. De Martino *et al.*, Phys. Rev. Lett. **88**, 206402 (2002).

[13] A. De Martino *et al.*, J. Phys. Condens. Matter **16**, S1437 (2004).

[14] J. C. Slater and J. F. Koster, Phys. Rev. **94**, 1498 (1954).

[15] D. Tománek and S. G. Louie, Phys. Rev. B **37**, 8327 (1988).

[16] X. Blase *et al.*, Phys. Rev. Lett. **72**, 1878 (1994).

[17] C. S. Wang and J. Callaway, Phys. Rev. B **9**, 4897 (1974); S. Gallego and M. C. Muñoz, Surf. Sci. **423**, 324 (1999).

[18] G. F. Dresselhaus, M. S. Dresselhaus, and J. G. Mavroides, Carbon **4**, 433 (1966).

[19] A. V. Moroz and C. H. W. Barnes, Phys. Rev. B **60**, 14 272 (1999); G.-H. Chen and M. E. Raikh, Phys. Rev. B **60**, 4826 (1999); M. Valín-Rodríguez, cond-mat/0404262.

[20] E. I. Rashba and Al. L. Efros, Phys. Rev. Lett. **91**, 126405 (2003).

[21] A. Kleiner and S. Eggert, Phys. Rev. B **63**, 73 408 (2001).

[22] Nanotubes are labeled by the numbers (n, m), given by the unrolled circumference vector $\boldsymbol{C}_h = n\mathbf{a}_1 + m\mathbf{a}_2$. The two lattice vectors of graphene at 60° are $\mathbf{a}_1$ and $\mathbf{a}_2$.

[23] If (n, m) are the nanotube indices, then for primary metallic nanotubes $n - m = 3q$, where q is an integer.

[24] Saito *et al.* (see, e.g., Ref. [1]) use the terms metal-1 and metal-2 with the same meaning.

[25] To classify a generic (n, m) tube, one has to compute the greatest common divisor (gcd) of (n, m) and $(2m + n, 2n + m)$. Let $d = \gcd(n, m)$ and $d_R = \gcd(2m + n, 2n + m)$. If $d_R = d$, the nanotube is a 2/3 metal, whereas if $d_R = 3d$, it is a Γ metal (see Ref. [1]).

[26] The point group of the (5,5) NT is D_{5d}. The corresponding irreducible representations are two 1D and four 2D. This allows us to classify the eigenvalues, yielding two nondegenerate and four doubly degenerate bands out of the ten conduction and ten valence bands.

[27] The point group of the (9,0) tube is D_{9d}. It has two 1D and eight 2D irreducible representations. Thus, out of the 18 conduction and 18 valence bands, only two are nondegenerate and eight are doubly degenerate.

[28] Chiral nanotubes have nonsymmorphic lattice groups. Their point groups are the abelian C_N groups; for the (7,1) tube $N = 38$, and for (9,3) $N = 78$. See Ref. [1] for details. In all cases the irreducible representations are either 2D or 1D.